Eur Biophys J (1993) 22:237–247

European Biophysics Journal

A site accessible to extracellular TEA^+ and K^+ influences intracellular Mg^{2+} block of cloned potassium channels

Uwe Ludewig [1], Christoph Lorra [2], Olaf Pongs [2], Stefan H. Heinemann [1]

[1] Max-Planck-Institut für biophysikalische Chemie, Abt. Membranbiophysik, D-37077 Göttingen, Germany
[2] Zentrum für molekulare Neurobiologie, D-20251 Hamburg, Germany

Received: 24 March 1993 / Accepted in revised form: 17 June 1993

Abstract. The members of the RCK family of cloned voltage-dependent K^+ channels are quite homologous in primary structure, but they are highly diverse in functional properties. RCK4 channels differ from RCK1 and RCK2 channels in inactivation and permeation properties, the sensitivity to external TEA, and to current modulation by external K^+ ions. Here we show several other interesting differences: While RCK1 and RCK2 are blocked in a voltage and concentration dependent manner by internal Mg^{2+} ions, RCK4 is only weakly blocked at very high potentials. The single-channel current-voltage relations of RCK4 are rather linear while RCK2 exhibits an inwardly rectifying single-channel current in symmetrical K^+ solutions. The deactivation of the channels, measured by tail current protocols, is faster in RCK4 by a factor of two compared with RCK2. In a search for the structural motif responsible for these differences, point mutants creating homology between RCK2 and RCK4 in the pore region were tested. The single-point mutant K533Y in the background of RCK4 conferred the properties of Mg^{2+} block, tail current kinetics, and inward ion permeation of RCK2 to RCK4. This mutant was previously shown to be responsible for the alterations in external TEA sensitivity and channel regulation by external K^+ ions. Thus, this residue is expected to be located at the external side of the pore entrance. The data are consistent with the idea that the mutation alters the channel occupancy by K^+ and thereby indirectly affects internal Mg^{2+} block and channel closing.

Key words: Potassium channel – Site-directed mutagenesis – Oocyte expression – Ion permeation – Mg block

Abbreviations: TEA, tetraethylammonium; EGTA, Ethylene glycol-bis (β-aminoethyl ether) N,N,N′,N′-tetraacetic acid; 2S3B model, 2-site 3-barrier model

Correspondence to: S. H. Heinemann

Introduction

Several ion channels are blocked by intracellular Mg^{2+} at physiological concentrations (for review see Hille 1992). In particular, inward rectifier potassium channels are strongly blocked by internal Mg^{2+} (e.g., Matsuda et al. 1987; Vandenberg 1987) but cloned voltage-dependent potassium channels from rat brain were also found to be blocked by physiological Mg^{2+} concentrations (Rettig et al. 1992). Here we show that some members of the family of potassium channels cloned from rat brain cortex (RCK family or Kv1 family according to the simplified notation by Chandy 1991) are blocked by millimolar concentrations of intracellular Mg^{2+} at high voltages while others are not. Although this voltage-dependent block by Mg^{2+} might only be of minor physiological relevance, the different blocking characteristics on quite homologous potassium channels offer a tool for structure-function studies of voltage-gated potassium channels.

The cloned voltage-gated potassium channels of the RCK family share a highly homologous primary structure, but they differ markedly in functional properties (Stühmer et al. 1988; 1989; Grupe et al. 1990). While RCK1 (Kv1.1) and RCK2 (Kv1.6) channels mediate classical delayed rectifier currents, the RCK4 (Kv1.4) channels inactivate in approximately 50 ms, and have about half the single-channel conductance ($\approx$5 pS) of RCK1 and RCK2 channels ($\approx$9 pS) in physiological solutions at 0 mV. Furthermore, in contrast to RCK1 and RCK2, RCK4 channels are quite resistant to blockage by extracellular tetraethylammonium (TEA) (Stühmer et al. 1989). RCK4 currents also depend strongly on extracellular K^+ ions (Pardo et al. 1992): the peak amplitude of outward K^+ current decreases with decreasing external K^+ concentration. This phenomenon has not been observed for RCK1 and RCK2, for example. While the sites responsible for the differences in single-channel conductance are still not known, the latter differences were related to the residues lysine (K533) and isoleucine (I535) in the extracellular loop between the transmembrane segments S5 and S6 of RCK4 channels by site-directed mutagenesis (Stocker

et al. 1991; Pardo et al. 1992). In Fig. 1 A the organization of the transmembrane segments S1–S6 and the pore region are shown. Part B illustrates a model of how the deep pore region of the potassium channels could be imagined to fold into the membrane to form part of the ion channel pore. The lysine residue of RCK4 (shaded K), which was assumed to be sufficient to account for the observed functional differences to both RCK1 and RCK2 (Pardo et al. 1992), is presumably located at the external entry of the deep pore region as suggested for other homologous potassium channel types (e.g., MacKinnon and Yellen 1990; Hartmann et al. 1991; Yellen et al. 1991; Kirsch et al. 1992). It should be noted that the residues K533 and I535 are the only differences between RCK4 and RCK2 in this region.

Here we show that the residue at position 533 in RCK4 is also responsible for differences in inward permeation of K^+, differences in the closing kinetics of various RCK channels, and the channel block by internal Mg^{2+}. Because this residue is accessible to external TEA and K^+, based on previous findings, it is interesting that it also determines the various intracellular Mg^{2+} block characteristics of several cloned RCK potassium channels. This suggests that both intra- and extracellular sites of ion interaction are influenced by this residue. We provide a possible explanation of this phenomenon based on a model for ion permeation through the RCK channels. All the observed differences in channel closing, block by internal Mg^{2+}, and inward K^+ permeation can be accounted for by a slight change of the external half of the energy profile of a two-site model for permeating K^+ ions and the resulting alteration in the channel occupancy of permeating ions. Such an effect would be expected for the introduction of mutations at an external pore site.

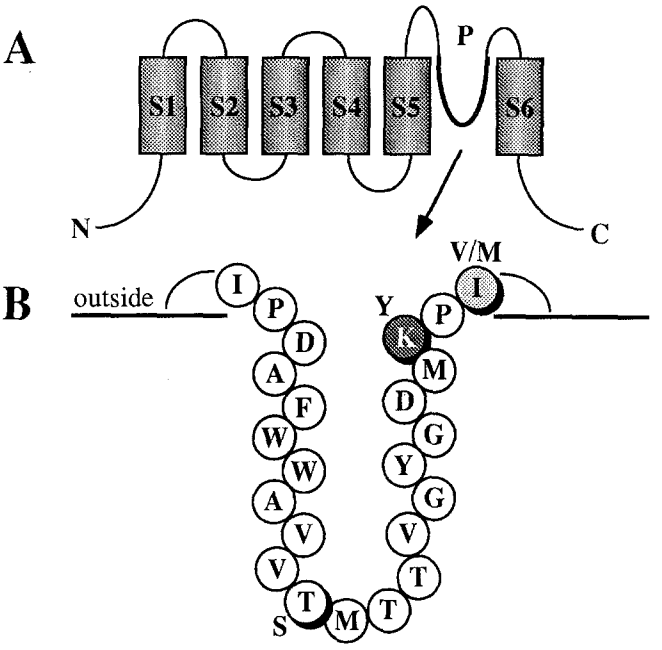

Fig. 1. **A** Model for the potassium channel protein with the six putative transmembrane segments S1–S6 and the pore region between S5 and S6 (segments not drawn to scale). **B** Topological model for the deep pore region, delimited by the two proline residues, of the RCK4 channel. The residues 513 through 535 are shown in single-letter code; differences with RCK1 (523S, 533Y, 535V) and with RCK2 (533Y, 535M) are indicated. The shaded residues were mutated in this study in order to eliminate differences between RCK4 and RCK2 in the pore region

Methods

Molecular biology

The RCK4-mutant K533Y · I535M was prepared as described by Stocker et al. (1991). The point mutation K533Y was introduced into RCK4-pAKS DNA (Stühmer et al. 1989) according to the method of Nelson and Long (1989) with modifications described in Stocker et al. (1991). The sequence of the reverse mutation primer was TGT GAT GGG ATA CAT GTC CCC. The mutated DNA was checked by sequencing and restriction analysis. For cRNA synthesis with SP6 polymerase (Krieg and Melton 1987) RCK1-pAKS, RCK2-pAKS, and RCK4-pAKS DNAs (Stühmer et al. 1989), and the mutant cDNAs were linearized with *Eco*RI.

Electrophysiology

RNA preparation and oocyte injection were performed as described previously (Methfessel et al. 1986; Stühmer et al. 1987). For heterologous expression of RCK channels, the specific cDNA-derived mRNA was injected into oocytes (average amount 25 pg per oocyte) and the currents were recorded 2–5 days after injection. Conventional patch-clamp techniques were used for the electrophysiological recordings. Macroscopic currents were measured in inside-out membrane patches with aluminium-silicate pipettes with resistances of 0.8–1.2 MΩ. For single-channel recordings we sometimes used smaller pipettes pulled from hard borosilicate glass with resistances of 5–10 MΩ. Leak and capacitive currents were subtracted on-line by using a variable P/n method with alternating polarity of the leak pulses (Heinemann et al. 1992). For single-channel recordings linear leak was subtracted off-line. Since RCK4 channels recover very slowly from inactivation, intervals of up to 1 min between pulses were chosen in those cases. For most measurements tail pulse protocols were used, starting from a holding potential of −100 mV and stepping after a prepulse to +140 mV to the test potential. Instantaneous current-voltage relations were constructed by fitting mono-exponential functions to the current traces in response to the voltage step after the prepulse. The extrapolated value at the beginning of the voltage step was used to construct current-voltage relations. The current-voltage relations of block were determined by taking the constant current after relaxation of the tail current to a constant value. Since reactivation of RCK4 channels is faster with elevated extracellular K^+ concentration (Pardo et al. 1992), unless otherwise specified, pipettes were filled for inside-out recordings with solution 1: 100 mM NaCl, 16 mM KCl, 10 mM Hepes, 1.8 mM $CaCl_2$, pH 7.2 (NaOH) or solution 2: 115 mM KCl, 10 mM Hepes, 1.8 mM

$CaCl_2$, pH 7.2 (KOH). The bath contained solution 3: 120 mM KCl, 10 mM Hepes, 1.8 mM EGTA, pH 7.2 (KOH) and varying amounts of $MgCl_2$ between 0 and 10.24 mM.

All electrophysiological experiments were performed at 19–21 °C. Pulse patterns were generated and currents were sampled with the *Pulse* software package (HEKA Electronik, Lambrecht, Germany) either on a VME-bus-based computer system with an EPC7 patch clamp amplifier (List Medical System, Darmstadt, Germany) or on a Macintosh IIfx computer with an EPC9 patch clamp amplifier (HEKA Electronik, Lambrecht, Germany). Before sampling data were passed through an 8-pole low-pass Bessel filter set to 10 kHz (−3 dB) unless otherwise stated.

Results

Block of RCK1 channels by intracellular Mg^{2+}

Intracellular Mg^{2+} blocks RCK1 channels in a voltage-dependent manner. Figure 2A shows macroscopic current recordings from an inside-out patch with 0 mM, 2.56 mM, or 10.24 mM Mg^{2+} in the bath solution. Macroscopic tail currents were recorded as response to voltage steps from the conditioning voltage of +140 mV to tail potentials ranging from −140 to +140 mV. Intracellular Mg^{2+} reduced the potassium current through RCK1 channels in a voltage-dependent manner, increasing the degree of block with increasing voltage. In 10.24 mM Mg^{2+} the small peak at the beginning of the conditioning pulse segment is indicative for the kinetics by which Mg^{2+} enters the channel. The gating currents are expected to contribute less than 2% of this signal. The high prepotential of +140 mV was chosen in order to visualize unblocking of the channels after steps to less positive potentials.

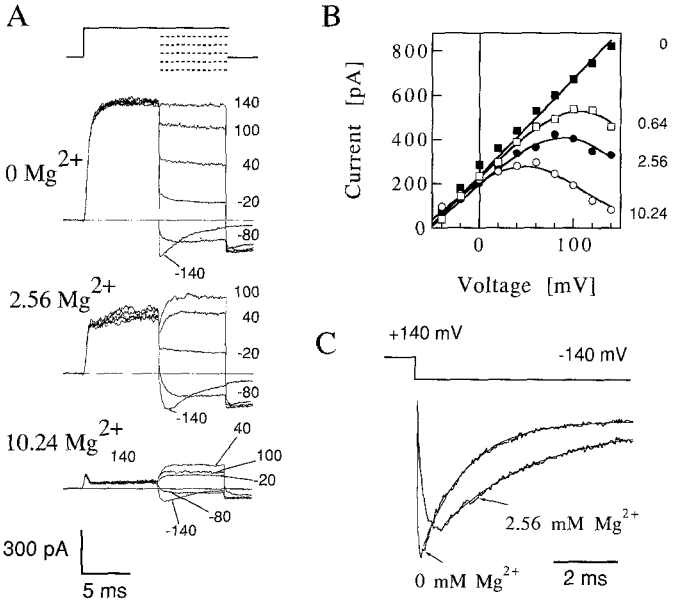

Fig. 2A–C. Intracellular Mg^{2+} blocks RCK1 potassium channels in a voltage and concentration dependent manner. **A** Macroscopic tail current recordings from inside-out patches without, with 2.56 mM, or with 10.24 mM Mg^{2+} in the bath. A conditioning pulse was given for 8 ms to 140 mV; the potentials of the tail segments are indicated in millivolts (mV). **B** Current-voltage relations for RCK1 channels in the indicated Mg^{2+} concentrations in mmol/l (mM). The continuous curves are data fits according to Eq. (1). **C** Tail current traces showing the relief of Mg^{2+} block at negative potentials. The superimposed curves are single-exponential data fits to the decaying current phase. External solution 1; internal solution 3 plus indicated Mg^{2+} concentration

RCK1 channels were blocked by different amounts of intracellular Mg^{2+} in a concentration-dependent manner. The current-voltage relations of outward currents in different Mg^{2+} concentrations were fitted with Eq. (1), which describes a simple voltage-dependent block (Woodhull 1973), assuming ohmic conductance of K^+ channels in the absence of Mg^{2+} (Pusch 1990):

$$I = \frac{g_k U}{1 + \frac{[Mg^{2+}]}{K_d(100\text{ mV})} \exp\left(\frac{\delta(U - 100\text{ mV})\, zF}{RT}\right)} \quad (1)$$

with the current I, conductance g_K, voltage U, magnesium concentration $[Mg^{2+}]$, half-maximal blocking concentration at 100 mV K_d(100 mV), electrical distance of the blocking site from inside δ, Faraday constant F, valence of the blocking ion z, general gas constant R, and absolute temperature T. The block is characterized by the half-maximal blocking concentration at 100 mV, K_d(100 mV) and the electrical distance from the internal surface, δ. K_d(100 mV) was defined by Eq. (2) with a voltage-independent dissociation constant of block, K_d(0 mV).

$$K_d(100\text{ mV}) = K_d(0\text{ mV}) \exp\left(-\frac{2\delta F(100\text{ mV})}{RT}\right). \quad (2)$$

In Fig. 2B current-voltage relations from RCK1 channels in different internal Mg^{2+} concentrations are shown. The data points were collected from current recordings from the same patch, where the bath medium was changed during the experiment. The curves in Fig. 2B were fitted simultaneously according to Eq. (1), holding g_k constant for all concentrations, since no rundown of channels was observed during the entire measurement. The concentration and voltage dependence of the block were determined from the average of 10 experiments, yielding $K_d(100\text{ mV}) = 5.0 \pm 1.3$ mM and $\delta = 0.32 \pm 0.15$. The voltage dependence corresponds to an e-fold increase in block of 39 mV.

The closing of the channels is also affected by internal Mg^{2+}. In Fig. 2C tail currents to −140 mV from RCK1 channels of the same patch in 0 and 2.56 mM Mg^{2+} are superimposed. The current trace in 2.56 mM Mg^{2+} differs from the one without Mg^{2+} in two respects: (a) the rising phase is indicative of a slow relief of Mg^{2+} block before the channels close and (b) the closing process appears to be slower. In Mg^{2+} solution the blocked channels do not close immediately after stepping to a negative potential. This gives rise to an increase in the current mediated by channels returning from a blocked state. The unblock kinetics followed an exponential function with a time con-

stant of approximately 200 μs at −140 mV. This phenomenon, together with the voltage-dependence of block, is consistent with Mg^{2+} ions acting directly inside the pore of these channels at a site that senses about 30% of the transmembrane electric field.

Even if one assumes that channels have to become unblocked before they can close (deactivate), the single-exponential current decay due to the closing of the channels was consistently slower by a about a factor of 2 in 2.56 mM internal Mg^{2+} solution. An explanation for this effect could be surface charge at the cytoplasmic side of the membrane due to elevated concentration of divalent cations. This would lower the potential drop across the membrane, affecting the voltage-dependent closing of the channels. By analysis of current-voltage relationships in respect to the half-activation potential such a voltage shift was estimated to be less than 10 mV by changing the internal solution from 0 to 2.56 mM Mg^{2+}. This potential shift would at most slow down the deactivation kinetics of the channels by a factor of 1.3 as judged from the potential dependence of deactivation (see also Fig. 7), leaving a net slowing of deactivation due to internal Mg^{2+}. This could be either due to a stronger effect of surface charge on deactivation than on activation or another as yet unknown specific effect of internal Mg^{2+} on the conformational change leading to channel deactivation.

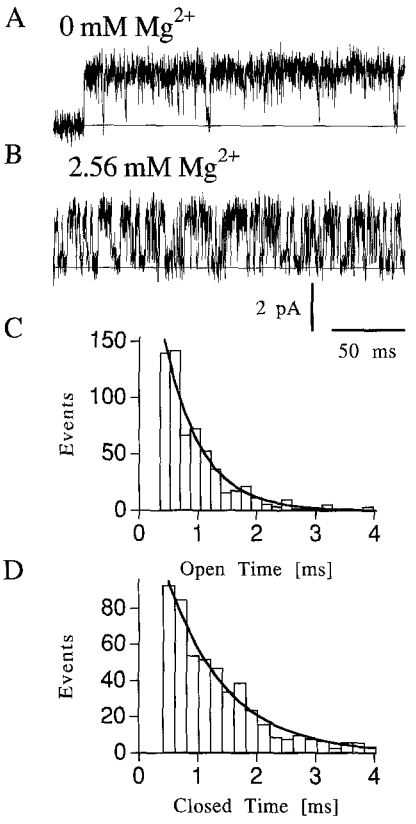

Fig. 3A–D. Flickering block of RCK1 channels by Mg^{2+}. **A** Single-channel currents without or **B** with 2.56 mM Mg^{2+} (external solution 1, internal solution 3) at 120 mV membrane potential. The currents were sampled at a rate of 20 kHz and filtered with an 8-pole low-pass Bessel filter at 4 kHz. **C** *Open* and **D** *closed time* histograms for data traces recorded in 2.65 mM internal Mg^{2+}. *Open times* between 3.7 ms and 320 ms and *closed times* between 3.7 ms and 400 ms were used. The calculated mean *open time* in these particular histograms was 0.64 ms and the mean *closed time* was 1.0 ms

Flickering block of RCK1 single-channel currents by intracellular Mg^{2+}

The time course of block at high positive potentials (see Fig. 2A) and of the relief from block after a step to negative potential suggests that single blocking events of Mg^{2+} ions should be resolvable in single-channel recordings despite the limiting bandwidth of the recording system.

Single-channel current recordings from RCK1 channels are shown in Fig. 3A, B. The traces show a flickering current, which represents the open (up) and shut (down) channel states, at 120 mV in the absence of Mg^{2+} (A) and with 2.56 mM Mg^{2+} (B) in the bath. In Mg^{2+} the closing events are much more frequent than in Mg^{2+}-free medium, where mostly long open times of the channel (often >100 ms) with short, unresolved closings are observed. These long open times are not seen in Mg^{2+} solution. In Mg^{2+} the current "flickers" suggest that Mg^{2+} ions close the channel completely for short times.

The observed gating behaviour in Mg^{2+}-free medium was described by Stühmer et al. (1988) as a gating mode of RCK1 channels with high open probability. Since RCK1 channels can also have a gating mode with lower open probability (Stühmer et al. 1988), we tested to see if the high open probability mode is also observed in the experiments using Mg^{2+} solutions. This was done by voltage steps to lower potentials, where the Mg^{2+} block is less prominent. Since the channels appear to switch rarely between different modes, the gating mode of the channels is unlikely to change after these voltage steps. At lower potentials long open times, indicating the high open probability mode, were also observed in Mg^{2+} medium (data not shown). This argues that the flickers at high voltages in Mg^{2+} solution are due to resolved closures of the channel by Mg^{2+} ions rather than by changes in the gating mode of the channels.

Open and closed time histograms were constructed from at least 300 ms long flickering current recordings. These histograms were well fit by single exponentials, which also adequately described the macroscopic unblocking of the channels after voltage steps to lower potentials (see rising phase of tail currents in Fig. 2C, for example). This favors a simple blocking mechanism with only two states of the activated channel, an open state and a blocked state. Histograms for the open and closed intervals at 120 mV are given in Fig. 3C and D. For 2.56 mM internal Mg^{2+} a mean open time of 0.83 ± 0.28 ms and a mean closed time of 1.1 ± 0.5 ms ($n = 5$) were determined.

RCK2 and RCK4 channels differ in their block by Mg^{2+}

Figure 4 illustrates the blocking effects of intracellular Mg^{2+} on two more members of the RCK channel family. RCK2 channels are blocked less than RCK1 (Fig. 2), as characterized by $K_d(100\text{ mV}) = 15.1 \pm 6.8$ mM and

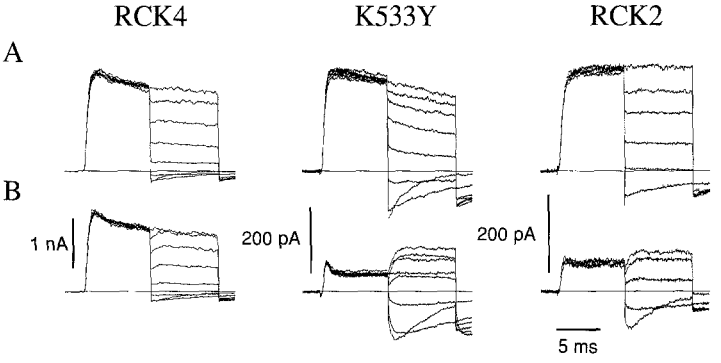

Fig. 4. Intracellular Mg^{2+} block of RCK4, the RCK4-based point mutant K533Y, or RCK2. Macroscopic tail currents without **A** or with **B** 10.24 mM Mg^{2+} from the same patch. RCK4 channels are only weakly blocked by internal Mg^{2+} while RCK2 channels show a block not quite as strong as RCK1 (see Fig. 2). The RCK4-based point mutant K533Y shows a Mg^{2+} block intermediate between RCK1 and RCK2. The protocol consisted of a conditioning pulse to +140 mV and subsequent tail pulse potentials ranging between −80 mV and +140 mV in steps of 40 mV. Filter: 8 kHz. External solution 1, internal solution 3

$\delta = 0.28 \pm 0.17$ (corresponding to 44 mV per e-fold block, $n = 43$). RCK4 channels are only significantly blocked at very high potentials and high Mg^{2+} concentrations. For example, compare the traces recorded from the same patches in part A (0 Mg^{2+}) and part B (10.24 mM Mg^{2+}) of Fig. 4 (also see Fig. 10C). However, at low Mg^{2+} concentration (up to 2.56 mM) the current-voltage relations of RCK4 channels were linear ($n = 11$). For RCK4 there is only a slight block at very high potentials and therefore almost no channels recovering from the blocked state are observed after stepping to lower potentials. Mg^{2+} is dragged into the channel only at very high potentials as seen in the small decrease of the current amplitude during the prepulse to +140 mV with Mg^{2+}. Thus, at the highest potentials the current-voltage relations deviate from a linear function (see also Fig. 10). The fit to the data according to Eq. (1) yielded K_d (100 mV) = 178 ± 41 mM and a voltage dependence of $\delta = 0.50 \pm 0.06$ ($n = 6$).

Kinetically, RCK4 channels are different from all other RCK channels because they inactivate quickly and recover slowly from inactivation. We therefore also checked for possible effects of internal Mg^{2+} on these parameters. Although internal Mg^{2+} did not affect inactivation properties the recovery from inactivation was slowed (data not shown). Unfortunately, this slowing of the reactivation kinetics could not be assayed in detail because the inactivation properties of RCK4 channels undergo changes in excised patches that are subject to regulation by the internal redox potential (Ruppersberg et al. 1991); RCK4 channels loose their fast inactivation in inside-out patches slowly after excision of the patch. The time course for the loss of fast inactivation, however, varies from patch to patch, presumably because of the variable kinetics for the washout of cytosolic substances from the inside-out patch area. Because the variability in the slow loss of inactivation together with the requirement of reactivation intervals of more than a minute for measurements of the time course of reactivation, a quantitative study of the slowing on the reactivation kinetics by internal Mg^{2+} was not feasible.

Localization of a site responsible for the differences in Mg^{2+} block

To determine the structural site responsible for the differences in block by intracellular Mg^{2+}, mutants of the RCK4 channel with amino-acid substitutions resembling the primary structures of RCK2 were assayed for Mg^{2+} block. Interestingly, one of the mutations (K533Y · I535M) changed the sensitivity of RCK4 to voltage-dependent block by intracellular Mg^{2+}. These mutations in RCK4 are sufficient to change the outer loop between the deep pore region and the putative transmembrane segment S6 into the RCK2 primary structure (Fig. 1). This mutant channel had a sensitivity to intracellular Mg^{2+} intermediate between RCK1 and RCK2 channels with K_d (100 mV) = 10.0 ± 4.0 mM and an electrical distance of 0.42 ± 0.03 ($n = 20$). Very similar characteristics were seen in the single-point mutant K533Y, where we measured K_d (100 mV) = 10.7 ± 1.1 mM and an electrical distance δ of 0.47 ± 0.07 ($n = 6$), as shown in Fig. 4 (center panel). In this mutant only the positively charged lysine residue of RCK4 is replaced by an uncharged tyrosine residue which is present in the equivalent position of both the RCK1 and RCK2 channels. Since voltage-gated potassium channels presumably consist of 4 subunits (MacKinnon 1991; Liman et al. 1992), the substitution of the lysine by tyrosine results in an overall decrease of 4 positive net charges in the functional channel protein.

Role of site 533 in RCK4 for several channel characteristics

TEA block and effect of external K^+

Recent work showed that the double mutation K533Y · I535M based on the RCK4 protein confers sensitivity to external TEA of RCK1 to RCK4 channels (Stocker et al. 1991) and that these residues play a crucial role in the sensitivity to channel modulation by extracellular K^+ (Pardo et al. 1992). Both effects were attributed to the lysine residue K533. This was confirmed here by measuring the external TEA block and the sensitivity to channel modulation by extracellular K^+ of the RCK4 mutant K533Y. This mutant has the same sensitivity to external TEA ($IC_{50} = 0.6 \pm 0.3$ mM, $n = 5$) as the double mutant K533Y · I535M (Stocker et al. 1991) and shows no dependence of peak current on external K^+, i.e., also in this respect K533Y has the same properties as the double mutant.

K^+ permeation

The permeation properties of RCK4 channels were also changed by the mutation. Most of the experiments were done on the double mutant K533Y · I535M, but the altered permeation characteristics were also seen in the point mutant K533Y. While the outward permeation was unchanged (Stocker et al. 1991), we observed that substitution of the lysine residue at position 533 by tyrosine alters the properties of RCK4 for inward K^+ permeation. This was most obvious in symmetrical high K^+ solutions.

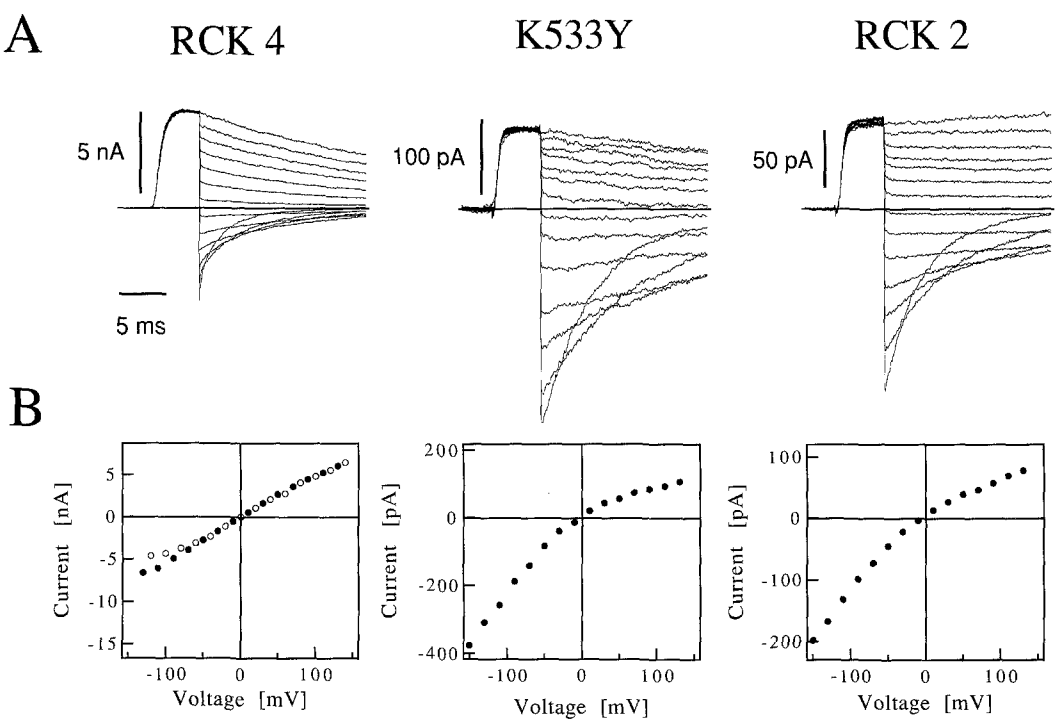

Fig. 5. **A** Macroscopic tail currents from RCK4, RCK4 mutant K533Y, or RCK2 channels in solutions with symmetrical high K^+ solutions (external solution: 2; internal solution: 3). **B** Instantaneous current-voltage relations from the traces in **A**. The mutant K533Y confers the inwardly rectifying characteristics of RCK2 on the RCK4 channel. The open symbols in the panel for RCK4 represent scaled data obtained in Ca^{2+}-free external solutions from a different patch indicating that the difference to RCK2 is not due to block by external Ca^{2+}

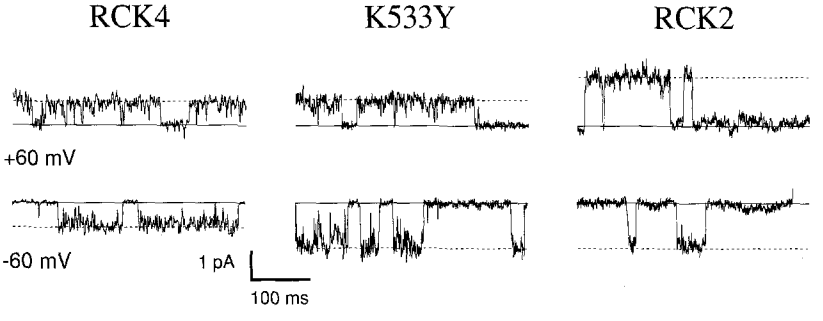

Fig. 6. Single-channel records at +/− 60 mV membrane potential from RCK4, RCK4 mutant K533Y, or RCK2 channels in solutions with symmetrical high K^+ (external solution: 2; internal solution: 3). The mutation K533Y conferred the inward current flow of RCK2 to RCK4 channels, while the outward current remained unchanged

In Fig. 5 instantaneous current-voltage relations of RCK4, the mutant K533Y, and RCK2 are shown. Although RCK4 channels have a nearly linear current-voltage relation, the mutation produces inwardly rectifying characteristics. However, the conductance in the positive voltage range is not changed in respect to RCK4 (Fig. 6). Inwardly rectifying current-voltage relations are also observed in RCK2 channels as well as in the mutant K533Y · I535M RCK4 channel.

Since inside-out patches were more stable with physiological external Ca^{2+} concentrations, the external medium contained 1.8 mM Ca^{2+} in most of the experiments. To find out whether the observed differences between RCK4 and RCK2 might be due to block of the inward currents through RCK4 channels by external Ca^{2+}, these experiments were repeated in Ca^{2+}-free medium. One current-voltage relation under these conditions is shown in Fig. 5B (open circles). Above −50 mV these current-voltage relations were indistinguishable from those in Ca^{2+}-containing solutions, suggesting that changes in the current-voltage relations between RCK4 and the mutant are due to altered K^+ permeation properties, rather than due to block by external Ca^{2+}. At lower potentials even a saturation in current was observed in Ca^{2+}-free solutions. This effect was not studied in greater detail.

In Fig. 6 single-channel events in symmetrical high K^+ are compared for RCK4, mutant K533Y, and RCK2 for +/−60 mV. Under these conditions the single-channel currents of RCK4 are smaller than those of RCK2 by about a factor of two in both directions. The single-point mutation confers the inward K^+ permeation of RCK2 on RCK4, leaving the outward permeation unchanged. This is an interesting result for the mutation makes the proposed deep pore region (the region between the proline residues in Fig. 1) identical to RCK2. This argues that the differences in the outward permeation of RCK2 and RCK4 channels are mediated by structural differences outside this region.

Deactivation kinetics

In Fig. 7 the time constants of closing, from experiments similar to those shown in Fig. 5A, are compared. The deactivation of the mutant RCK4 channels (K533Y · I535M and K533Y, open squares) was slightly slower than RCK2 channels (filled squares) and thereby clearly differed from the deactivation of RCK4 channels (filled circles). The deactivation of RCK4 is about twice as fast as that of RCK2 and the mutant channels in the voltage range explored. Thus, the mutated site (533) also influences the gating of these channels. RCK4 and K533Y · I535M do not differ in respect to activation kinetics (also see Pardo et al. 1992, Fig. 2).

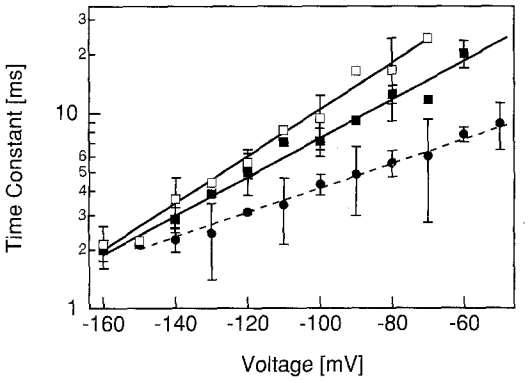

Fig. 7. Time constants for channel deactivation after a conditioning pulse to +130 mV in symmetrical high K^+ solutions (external solution: 2; internal solution: 3) are plotted as function of the test potential. Throughout the explored potential range RCK4 channels (*filled circles*) deactivate faster than RCK2 channels (*filled squares*) by a factor of approximately two. The *open squares* represent the pooled time constants for point mutants K533Y and K533Y · I535M

Model of ion permeation

As described above, a single-point mutation in the pore region of RCK4 channels alters ion permeation, block by internal Mg^{2+} and the kinetics of channel deactivation. Further insight, into the potential mechanisms behind these effects, may be gained by attempting a formal description of the ion flow through the channel. In order to constrain a quantitative permeation model, instantaneous current-voltage relations were measured in three different external K^+ concentrations and, in addition, single-channel amplitude measurements were obtained at these concentrations over a wide voltage range. Single-channel data were used to scale the instantaneous current-voltage relations to single-channel amplitudes. These scaled current-voltage relations were then used for simultaneous fits to a simple permeation model. This model describes all of the observed effects based on altered channel occupancy caused by the point mutation in the pore.

Potassium ion flux through the pores of RCK channels was modeled as single-file transport assuming an energy profile with 2 binding sites and 3 barriers (2S3B) allowing for double channel occupancy of K^+ (Hille and

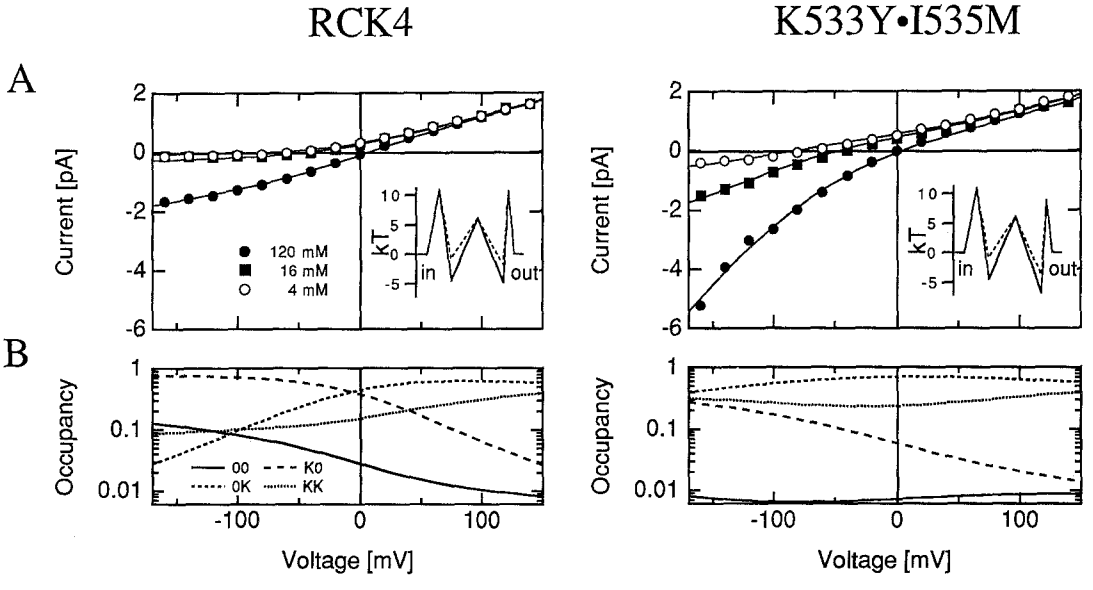

Fig. 8A–B. Permeation model with two sites and three barriers. **A** Single-channel current-voltage relations recorded with the indicated external K^+ concentrations of the RCK4-based mutant K533Y · I535M channels (*right panel*) were fit by a 2S3B permeation model. The fit to the data obtained for RCK4 (*left panel*) was done by taking the parameters from the data fit to the mutant and leaving only the external barrier and binding site free to vary. Schemes for the energy in units of kT as function of the relative position inside the electric field across the channel pore are shown as insets assuming a K^+ concentration of 1 M and 0 mV membrane potential. The *solid lines* represent the energy profile for a singly occupied channel, the *dashed lines* indicate the energies if both sites are occupied by K^+ ions. The relative electrical distances of the binding sites were in both cases 0.28 and 0.87 from the inside. The state diagram for K^+ permeation through K533Y was the same as the left part of Fig. 10A. **B** Probability of site occupancy for the permeation models in **A** assuming symmetrical 120 mM K^+ as a function of membrane potential; RCK4 is more likely to be unoccupied (00, *solid line*) than is the mutant. *Long dashes:* probability for internal site being occupied (K0); *short dashes:* probability for external site being occupied (0K); *dots:* probability for both sites being occupied (KK)

Schwartz 1978). Although there may be many good reasons for supposing that the mechanism of K^+ permeation requires more sophisticated approaches for modeling, such as to account for the diffusion of ions inside the channel (e.g., Gates et al. 1990) or to introduce more than two binding sites, we restricted this analysis to two binding sites and an Eyring rate theory approach (Eyring et al. 1949) in order to minimize the number of free parameters. A relation between the rate for barrier crossing, k, and the height of the energy barrier, ΔG, is assumed to be approximated by Eq. (3):

$$k = \frac{k_B T}{h} \exp\left(-\frac{\Delta G}{k_B T}\right) \quad (3)$$

with Boltzmann's constant k_B and Planck's constant h. It should be noted that only the relative values of the ΔG's reflect a physical meaning in such barrier models because of the rather arbitrary frequency factor $k_B T/h$. The state diagram for K^+ transport is shown on the left side of Fig. 10 A. Methods for the calculation of the current as a function of voltage, as well as the data fit algorithms, were used as described previously (Heinemann and Sigworth 1988).

Despite the gross simplifications introduced by such a model, the permeation of potassium ions through these channels could be well described. Because of the large number of free parameters we constrained the fit to the data obtained from RCK4; the rationale being that the effects of the site 533 on external TEA blockage and current modulation by external K^+ strongly suggest that this site is accessible from the external side of the channel. We therefore assumed that the internal half of the energy profile for K^+ permeation is not going to be changed by the mutation K533Y. Therefore, the first step of the analysis consisted of a free fit of the permeation model to all the data obtained for mutant K533Y · I535M yielding a description represented by the current-voltage relationships shown in Fig. 8 A (right panel). The data for K533Y are identical to those of K533Y · I535M so that the same model parameters were used for both. Starting from the fit parameters obtained for the mutant channels we therefore only varied the external binding site and the external barrier height, leaving the rest of the energy profile constant, in order to fit the RCK4 data as shown in Fig. 8 A (left panel). In the insets of Fig. 8 A the energy profiles for both cases are shown for the standard situation: 1 M K^+ and vanishing membrane potential with the dashed lines representing the profiles for doubly occupied channels. A decrease of the external barrier for entering ions by 1.25 kT and an increase of the barrier from the external to the internal binding site by 2.03 kT was sufficient to account for the changes introduced by the replacement of Lys by Tyr at position 533 in RCK4. This supports the physical picture that the mutation affects the external area of the ion pore since the data can be described without interference of this residue with the internal binding site for K^+. All parameters of the data fit are given in Fig. 10.

The probability for channel occupancy is shown in Fig. 8 B. As expected from the different current-voltage relationships, channel occupancy of K^+ differs between RCK4 and K533Y · I535M. In particular at negative potentials the probability of the channel being empty (solid line) is much higher for RCK4 than for K533Y · I535M.

Internal Mg^{2+} block depends on external K^+

The effects on internal Mg^{2+} block reported here along with the effects reported for external TEA^+ block and K^+ sensitivity (Stocker et al. 1991; Pardo et al. 1992) as a function of the residue at position 533 in RCK4 channels suggest that this residue has an influence on channel characteristics thought to be located on both the internal and external sides of the membrane. The alterations in internal Mg^{2+} block could be due to direct modification of the Mg^{2+} binding site or due to indirect effects resulting from an altered pore occupancy with K^+ ions. If the changed

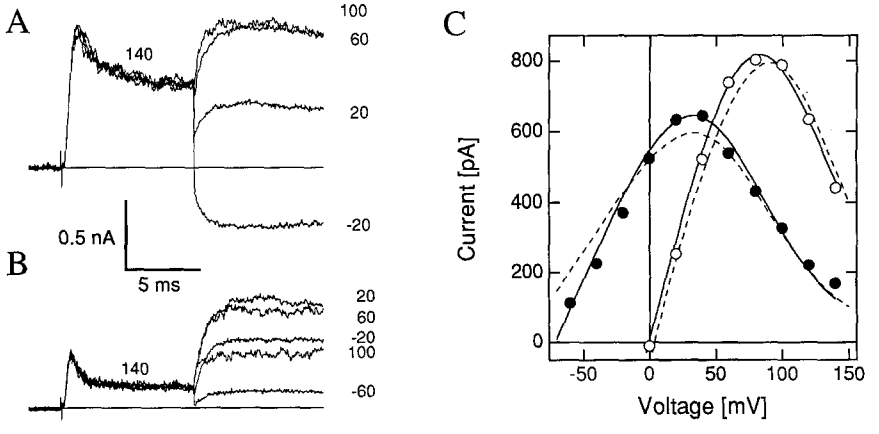

Fig. 9 A–C. The intracellular Mg^{2+} block of the RCK4 mutant K533Y is modulated by external K^+ ions. **A** Macroscopic tail currents from an outside-out patch at the indicated potentials (in mV) with internal 10.24 mM Mg^{2+} and symmetrical high K^+ (external solution: 2 internal solution: 3). **B** Macroscopic tail currents with internal 10.24 mM Mg^{2+} and 115 mM K^+, and external 2.5 mM K^+ from the same patch as in **A**. **C** Current-voltage relations of the asymptotic values of the tail currents obtained from the records in **A** and **B** (*filled circles:* 2.5 mM K^+, *open circles:* 115 mM K^+). The *continuous lines* represent the data fit according to Eq. (1). The *dashed lines* represent the fit according to the microscopic 6 state model as described in the text and in Fig. 10

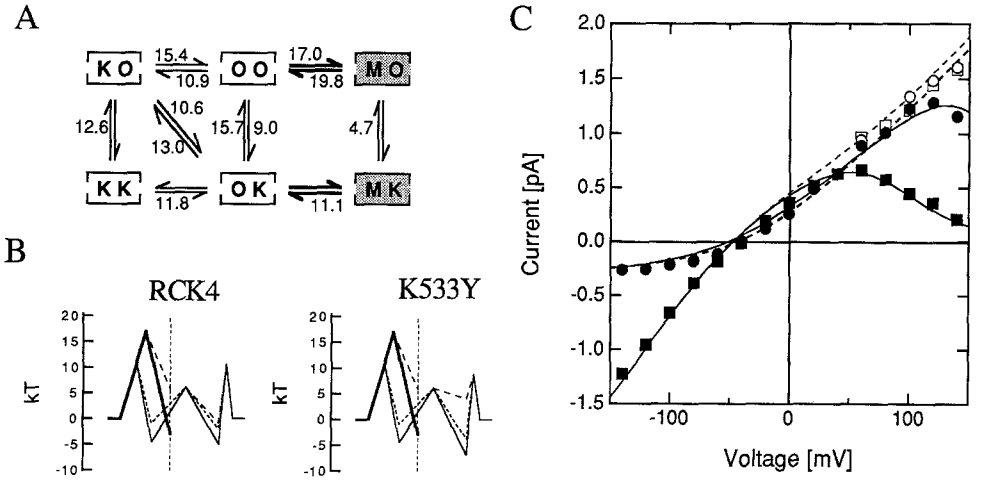

Fig. 10. **A** State diagramm for ion permeation and channel block by Mg^{2+}. The boxes represent a channel with two binding sites, the left one corresponds to the internal site. The values at the transition arrows indicate the energies in units of kT that have to be overcome for mutant K533Y. The states involving channel block by Mg^{2+} are shown in gray, the rates involving Mg^{2+} transport are indicated by thick arrows. The data for RCK4 were fit by a model where only rate constants into and out of the external binding site were altered in respect to K533Y. In units of kT these energies were: 00 → 0K: 11.3; 0K → 00: 15.5; 0K → K0: 11.0; KK → 0K: 12.6; MK → M0: 11.3. **B** Energy profiles for RCK4 and the point mutant K533Y including the energy barrier for Mg^{2+}. *Thin solid:* 0K or K0, *short dashes:* KK, *thick solid*: M0, *long dashes*: MK. The *vertical dashed lines* indicate the binding site for Mg^{2+}; note that Mg^{2+} cannot leave the channel to the right (to outside). **C** Current as a function of potential from raw data as shown in Fig. 4 for RCK4 (*circles*) and K533Y (*squares*) without (*open symbols*) or with 10.24 mM internal Mg^{2+} (*filled symbols*). External solution 1, internal solution 3 were used. The curves are predictions of the permeation and block model as shown in **A** and **B**. The model was not constrained for microscopic reversibility in order to account for small deviations of the local K^+ concentration after conditioning pulses from the bulk concentrations, which were used for the calculations

blocking characteristics were due to indirect pore occupancy effects, increased external K^+ concentration should increase the K^+ occupancy of the channel and should therefore reduce the block by internal Mg^{2+}. To test this hypothesis, the external K^+ concentration was varied with the mutant channel K533Y in an attempt to restore the insensitivity of RCK4 channels to intracellular Mg^{2+} block. These experiments showed that the internal Mg^{2+} block is highly sensitive to external K^+ concentration (Fig. 9).

Increasing external K^+ concentration led to a reduction of internal block by Mg^{2+}. The block parameters obtained for the different concentrations are shown in Table 1. While for different external K^+ concentrations the electrical distance δ for the block was constant, K_d (100 mV) varied threefold between zero and 115 mM external K^+.

Table 1. Effect of external K^+ on internal Mg^+ block

$[K^+]_0$	0 mM	2.5 mM	16 mM	115 mM
K_d (100 mV)	3.5 ±1.2	3.0 ±0.6	10.8±1.0	10.1±3.8
δ	0.41±0.03	0.40±0.06	0.45±0.05	0.44±0.03
n	3	4	4	7

Parameters of block of K533Y by internal Mg^{2+} in the indicated external potassium concentrations, $[K^+]_0$. Internal solution: 3 plus 10.24 mM $MgCl_2$

A model for Mg^{2+} block of cloned potassium channels

The Mg^{2+} block was described on the basis of the model for potassium permeation in RCK channels. One binding site for Mg^{2+} 40% inside the transmembrane electric field from the cytoplasmic side was assumed. In the microscopic state diagram channel block by Mg^{2+} was accounted for by the introduction of two more states (shown as gray boxes): M0 and MK, two blocked states, one in which the pore is occupied by a single Mg^{2+} and the other, where the pore binds K^+ and Mg^{2+} simultaneously (Fig. 10A). Because the location of the Mg^{2+} binding site, inside the electric field, is similar to the location of the internal binding site for K^+, it was assumed, that the internal sites for Mg^{2+} and K^+ could not be occupied simultaneously. The parameters for K^+ permeation in this 6 state model were taken from the fits as shown in Fig. 8.

The data for Mg^{2+} blockage of mutant K533Y in different external K^+ concentrations was fit with two assumptions: 1) the entrance of K^+ into the channel from one side is independent of the occupancy of the binding site on the opposite side of the pore and 2) starting values for the blocking rates on the order of those determined for RCK1 channels were used. The best fit is shown in Fig. 10 and as dashed lines in Fig. 9. Since the mutated site probably lies on the external pore mouth, only the exit rate for K^+ should be different between RCK4 wild-type and mutant channels. The rates involving transport of Mg^{2+} were left unchanged; the exit rate of K^+ from channels occupied by Mg^{2+} was therefore fit to the RCK4 Mg^{2+} data. The result is shown in Figs. 9 and 10. This model shows how the differential Mg^{2+} block of RCK4 and mutant K533Y can be explained by the different exit rates

for K^+ ions out of the channel, while the channel is occupied by a Mg^{2+} ion without affecting the microscopic rates by which Mg^{2+} crosses the energy barriers into and out of the channel. It is an example for how a residue remote from an actual binding site can influence the occupancy of that site in an indirect way.

Discussion

The channels of the RCK family differ markedly in their functional properties. Many of these differences can be attributed to the residue at position K533 in RCK4 channels. At the homologous position both RCK1 and RCK2 have a tyrosine residue. This tyrosine is responsible for their sensitivity to external TEA. At the same time these channels are not modulated by external K^+ ions while RCK4 currents disappear when external K^+ is removed. Here we have shown that inward ion permeation, channel deactivation kinetics, and channel block by internal Mg^{2+} also depend on the amino-acid that site. The homologous site in *Shaker* B potassium channels (T449) was previously shown to affect ion permeation (MacKinnon and Yellen 1990). The site I535 in RCK4 seems to be of minor importance for these phenomena.

If the deep pore region of RCK4 is made identical to RCK2 by the mentioned point mutations, the inward K^+ permeation of RCK2 is conferred on RCK4. The outward current, however, is not changed, indicating that the permeation in these channels is not solely mediated by this region. It is conceivable that residues connecting the segments S4 and S5 take part in forming the inner part of the channel funnel and thereby determine outward ion flow as proposed by the model of Guy and collaborators (e.g., Durell and Guy 1992).

Since mutation of the site 533 has effects on external TEA binding and external K^+ dependence, it is assumed that the site is easily accessible from the external side of the channel. In current models it is located at the external entry of the deep pore (Fig. 1). Channel deactivation and block by internal Mg^{2+} are processes that presumably involve part of the channel that are located near the inside of the pore and should therefore not be directly affected by mutation of the site K533. A possible explanation could therefore be that the changed inward permeation is a direct effect of the mutation on K^+ permeation while the altered deactivation kinetics and Mg^{2+} block are indirectly affected through channel occupancy of permeating ions. Correlations between channel occupancy of ions and gating properties were observed for various potassium channels (e.g., Demo and Yellen 1992; Matteson and Swenson 1986; Sala and Matteson 1991; Swenson and Armstrong 1981).

To test this hypothesis, we tried to model ion permeation through the RCK channels using an Erying approach. Although it is conceivable that there can be up to three K^+ ions in the potassium channel at a time, we restricted our model to three energy barriers and two binding sites in order to reduce the degrees of freedom. Ion permeation through the RCK4-based mutants K533Y and K533Y · I535M could be well described by such a model. Only the external energy barrier and binding site of this parameter set had to be adjusted to yield a description of ion permeation through RCK4: well reflecting the potential physical change introduced by these mutations.

The different energy profiles in the wild-type and mutant channels induce different pore occupancies for permeating K^+ ions. The altered voltage-dependent deactivation may therefore be a direct effect induced by the mutation, however, it may also be an indirect effect resulting from the varied occupancy of the channels by K^+ ions. Our model cannot state clearly by which mechanism the point mutation slows down deactivation. Judging from the channel occupancies of Fig. 8 B the signficantly higher probability of empty RCK4 channels could indicate that channels that are not occupied by ions tend to deactivate faster. This is consistent with previous results obtained for related potassium channels (e.g., Demo and Yellen 1992; Matteson and Swenson 1986; Sala and Matteson 1991; Swenson and Armstrong 1981).

The differential block by internal Mg^{2+} could be well described by a permeation model with one additional binding site for Mg^{2+}. In this model the channel can be occupied simultaneously by two ions, K^+ and Mg^{2+}, which bind at different sites inside the electric field across the membrane. The internal binding site for K^+ can only be occupied, if no Mg^{2+} is in the channel. In this framework the change in *internal* Mg^{2+} block induced by the mutation K533Y could be explained through alterations in the energy profile at the *external* side of the pore. These results clearly demonstrate the need to analyze carefully the permeation mechanism when conclusions are drawn about the location and the role of residues in interactions with other residues or applied test molecules (e.g., blockers) even when restricted to one side of the membrane.

Block by internal Mg^{2+} ions was used as an assay to distinguish biophysical properties of different members of the RCK channel family. The observed differences could be attributed to a single amino-acid residue at the external entry of the deep pore. Mutation of this residue modifies channel occupancy by permeating ions and could thereby control other channel parameters that depend on ion occupancy such as channel deactivation and block by internal Mg^{2+}. Thus, this study shows that there can be close relationships between channel gating and ion permeation. This is of particular importance for processes like deactivation (e.g., Swenson and Armstrong 1981) and C-type inactivation (López-Barneo et al. 1993) as well as for open-channel block by toxins or divalent ions.

Acknowledgements. We would like to thank Drs. K. McCormack and F. J. Sigworth for suggestions about the manuscript.

References

Chandy KG (1991) Simplified gene nomenclature. Nature 352:26

Demo A, Yellen G (1992) Ion effects on gating of the Ca^{2+}-activated K^+ channels correlate with occupancy of the pore. Biophys J 62:639–649

Durell SR, Guy HR (1992) Atomic scale structure and functional models of voltage-gated potassium channels. Biophys J 62:238–250

Eyring H, Lumry R, Woodbury JW (1949) Some applications of modern rate theory to physiological systems. Rec Chem Prog 10:100–114

Gates P, Cooper K, Rae J, Eisenberg R (1990) Predictions of diffusion models for one-ion membrane channels. Prog Biophys Molec Biol 53: 153–196

Grupe A, Schröter KH, Ruppersberg JP, Stocker M, Drewes T, Beckh S, Pongs O (1990) Cloning and expression of a human voltage-gated potassium channel. A novel member of the RCK potassium channel family. EMBO J 9:1749–1756

Hartmann HA, Kirsch GE, Drewe JA, Taglialatela M, Joho RH, Brown AM (1991) Exchange of conduction pathways between two related K^+ channels. Science 251:942–944

Heinemann SH, Sigworth FJ (1988) Open channel noise IV. Estimation of rapid kinetics of formamide block in gramicidin A channels. Biophys J 54:757–764

Heinemann SH, Conti F, Stühmer W (1992) Recording of gating currents from *Xenopus* oocytes and gating noise analysis. In: Rudy B, Iverson LE (eds) Ion channels, Methods in Enzymology, vol 203. Academic Press, San Diego, pp 353–368

Hille B (1992) Ionic channels of exitable membranes. Sinauer Associates INC., Sunderland, Massachusetts

Hille B, Schwartz H (1978) Potassium channels as multi-ion single-file pores. J Gen Physiol 72:409–442

Kirsch GE, Drewe JA, Hartmann HA, Taglialatela M, de Biasi M, Brown AM, Joho RH (1992) Differences between the deep pores of K^+ channels determined by an interacting pair of nonpolar amino acids. Neuron 8:499–505

Krieg PA, Melton DA (1987) In vitro RNA synthesis with SP6 RNA polymerase. Methods Enzymol 155:397–415

Liman ER, Tytgat J, Hess P (1992) Subunit stoichiometry of a mammalian K^+ channel determined by construction of multimeric cDNAs. Neuron 9:861–871

López-Barneo J, Hoshi T, Heinemann SH, Aldrich RW (1993) Effects of external cations and mutations in the pore region on C-type inactivation of *Shaker* potassium channels Rec Channels 1:61–71

MacKinnon R (1991) Determination of the subunit stoichiometry of a voltage-activated potassium channel. Nature 350:232–235

MacKinnon R, Yellen G (1990) Mutations affecting TEA blockade and ion permeation in voltage-activated K^+ channels. Science 250:276–279

Matsuda H, Saigusa A, Irisawa H (1987) Ohmic conductance through the inwardly rectifying K channel and blocking by internal Mg^{2+}. Nature 325:156–159

Matteson DR, Swenson RP (1986) External monovalent cations that impede the closing of K channels. J Gen Physiol 87:795–816

Methfessel C, Witzemann V, Takahshi T, Mishina M, Numa S, Sakmann B (1986) Patch clamp measurements on *Xenopus Oocytes*: currents through endogenous channels and implanted acetylcholine receptor and sodium channels. Pflügers Arch 407: 577–588

Nelson RM, Long GL (1989) A general method of site-specific mutagenesis using modification of the *Thermus aquaticus* polymerase chain reaction. Anal Biochem 180:147–151

Pardo LA, Heinemann SH, Terlau H, Ludewig U, Lorra C, Pongs O, Stühmer W (1992) Extracellular K^+ specifically modulates a rat brain K^+ channel. Proc Natl Acad Sci, USA 89:2466–2470

Pusch M (1990) Open-channel block of Na^+ channels by intracellular Mg^{2+}. Eur Biophys J 18:317–326

Rettig J, Wunder F, Stocker M, Lichtinghagen R, Mastiaux F, Beckh S, Kues W, Pedarzani P, Schröter KH, Ruppersberg JP, Veh R, Pongs O (1992) Characterization of a *Shaw*-related potassium channel family in rat brain. EMBO J 11:2473–2486

Ruppersberg JP, Stocker M, Pongs O, Heinemann SH, Frank R, Koenen M (1991) Regulation of fast inactivation of cloned mammalian I_k (A) channels by cysteine oxidation. Nature 352:711–714

Sala S, Matteson DR (1991) Voltage-dependent slowing of K channel closing kinetics by Rb^+. J Gen Physiol 98:535–554

Stocker M, Pongs O, Hoth M, Heinemann SH, Stühmer W, Schröter KH, Ruppersberg JP (1991) Swapping of functional domains in voltage-gated K^+channels. Proc R Soc London, Ser B 245:101–107

Stühmer W, Methfessel C, Sakmann B, Noda M, Numa S (1987) Patch clamp characterization of sodium channels expressed from rat brain. Eur Biophys J 14:131–138

Stühmer W, Stocker M, Sakmann B, Seeburg P, Baumann A, Grupe A, Pongs O (1988) Potassium channels expressed from rat brain cDNA have delayed rectifier properties. EMBO J 8:3235–3244

Stühmer W, Ruppersberg JP, Schröter KH, Sakmann B, Stocker M, Giese KP, Perschke A, Baumann A, Pongs O (1989) Molecular basis of functional diversity of voltage-gated potassium channels in mammalian brain. FEBS Lett 242:199–206

Swenson RP, Armstrong CM (1981) K^+ channels close more slowly in the presence of external K^+ and Rb^+. Nature 291:427–429

Vandenberg CA (1987) Inward rectification of a potassium channel in cardiac ventricular cells depends on internal magnesium ions. Proc Natl Acad Sci, USA 84:2560–2564

Woodhull AM (1973) Ionic blockage of sodium channels in nerve. J Gen Physiol 61:687–708

Yellen G, Jurman ME, Abramson T, MacKinnon R (1991) Mutations affecting internal TEA blockade identify the probable pore-forming region of a K^+ channel. Science 251:939–942